Hindawi Publishing Corporation
Journal of Nanomaterials
Volume 2015, Article ID 908689, 10 pages
http://dx.doi.org/10.1155/2015/908689

Research Article

Effects of Two Different Cellulose Nanofiber Types on Properties of Poly(vinyl alcohol) Composite Films

Kitti Yuwawech,[1,2] Jatuphorn Wootthikanokkhan,[1,2] and Supachok Tanpichai[1,3]

[1] *Nanotec-KMUTT Center of Excellence on Hybrid Nanomaterials for Alternative Energy, King Mongkut's University of Technology Thonburi (KMUTT), Thonburi, Bangkok 10140, Thailand*
[2] *School of Energy, Environment and Materials, King Mongkut's University of Technology Thonburi (KMUTT), Bangkok 1014, Thailand*
[3] *Learning Institute, King Mongkut's University of Technology Thonburi (KMUTT), Bangkok 10140, Thailand*

Correspondence should be addressed to Jatuphorn Wootthikanokkhan; jatuphorn.woo@kmutt.ac.th

Received 2 December 2014; Revised 27 January 2015; Accepted 28 January 2015

Academic Editor: Alain Dufresne

This work concerns a study on the effects of fiber types and content of cellulose nanofiber on mechanical, thermal, and optical properties polyvinyl alcohol (PVA) composites. Two different types of cellulose nanofibers, which are nanofibrillated cellulose (NFC) and bacterial cellulose (BC), were prepared under various mechanical treatment times and then incorporated into the PVA prior to the fabrication of composite films. It was found that tensile modulus of the PVA film increased with nanofibers content at the expense of its percentage elongation value. DSC thermograms indicate that percentage crystallinity of PVA increased after adding 2–4 wt% of the fibers. This contributed to the better mechanical properties of the composites. Tensile toughness values of the PVA/BC nanocomposite films were also superior to those of the PVA/NFC system containing the same fiber loading. SEM images of the composite films reveal that tensile fractured surface of PVA/BC experienced more ductile deformation than the PVA/NFC analogue. The above discrepancies were discussed in the light of differences between the two types of fibers in terms of diameter and their intrinsic properties. Lastly, percentage total visible light transmittance values of the PVA composite films were greater than 90%, regardless of the fiber type and content.

1. Introduction

Cellulose, a linear chain polysaccharide of β-(1→4)-D-glucopyranose units, is one of the most abundant natural biopolymers in the world [1–3]. Cellulose nanofibers such as nanofibrillated cellulose (NFC) and bacterial cellulose (BC) have attracted more and more interest as reinforcement in polymers due to their superior mechanical properties, higher aspect ratio, higher crystallinity, and lower coefficient thermal expansion, compared to micron sized cellulose fibers [4–10]. NFC can be produced from both cellulose I source, such as wood fibers, cotton, and agricultural crops, and cellulose II source such as lyocell fibers using various techniques such as grinding, high pressure homogenization, and sonication [1, 3, 11–13]. NFC is a high aspect ratio cellulose fibril with diameters of 10–100 nm and with lengths of tens of microns [3, 11, 12, 14–16]. Alternatively, another type of nanocellulose can be produced by the fermentation of sugar by the Gram-negative bacteria Acetobacter xylinumor *Gluconacetobacter xylinus* sources [5, 6, 17, 18]. This type of the cellulose material is known as bacterial cellulose (BC). The diameters of BC nanofibers are in the range of 25–200 nm [19]. The effective modulus of BC filaments investigated using Raman spectroscopy [17, 20] and atomic force microscopy [18] has been reported to be in the range of 79–114 GPa, which is close to a value of 138 GPa for the crystal modulus of cellulose I [21, 22]. This is due to its higher degree of crystallinity.

NFC and BC have been regarded as the next renewable reinforcements for the production of high performance biocomposites. Both NFC and BC fibrils have been significantly used to reinforce a wide range of polymers, such as poly(lactic acid) [5, 10, 11, 14], polypropylene [13], acrylic resin [23], polycaprolactone [24], poly(vinyl acetate) [25], and poly(vinyl alcohol) [26], to name a few examples, to make

composites with enhanced mechanical properties. Quero et al. [5] prepared BC reinforced poly(lactic acid) composites using compression molding. The tensile strength and Young's modulus of the PLA composites, containing 18% volume fraction of BC fibers, were found to increase by 315% and 100% to 218 MPa and 13 GPa, respectively, compared to neat poly(lactic acid) resin. The presence of BC fibril in a polymer can also induce crystallization of the polymer. BC pellicles compressed into sheets were also impregnated with phenolic resin to produce high-strength composites [18]. Tensile strength and Young's modulus of the BC reinforced composites, at an equivalent fiber weight fraction of 87.6%, were enhanced to be 425 MPa and 28 GPa, respectively. NFC has also been found to enhance the mechanical properties of several polymers. Polypropylene composites, reinforced with NFC (10 wt%), were prepared using a compression molding. The improvement of 45% and 52% of Young's modulus and tensile stress, compared to those of neat polypropylene, was reported, and NFC was also found to act as nucleating agent in the polypropylene matrix [13]. Iwatake et al. [14] studied mechanical properties of NFC reinforced poly(vinyl alcohol) (PVA) film and found that tensile strength of the solution casted nanocomposite film is two times higher than that of neat PVA. Young's modulus and tensile strength of PLA were increased by 40% and 25%, respectively, without reduction of yield strain after 10 wt% of NFC was added.

Even though the diameters of both BC and NFC are considerably low (less than 100 nm) [27], purity and crystal structure of the two cellulose nanofibers are different. BC is essentially pure cellulose, whereas the NFC consists of cellulose, hemicelluloses, and pectin. Two different crystal structures exist in the semicrystalline phase of cellulose, that is, cellulose I_α and cellulose I_β. BC is cellulose I_α rich, whereas plant based NFC is I_β rich. In this regard, it is interesting to compare the reinforcing efficiency of both nanocellulose fibers in polymer composites. Lee et al. [19] showed that mechanical properties of epoxy nanocomposites containing BC can be different from that of NFC reinforced epoxy composite, depending on the fiber loading. Nakagaito et al. [18] also studied mechanical properties of phenolic resin reinforced with BC sheet and found that Young's modulus of the composites was significantly higher than that of NFC-based composites (28 GPa against 19 GPa, resp.). Lee et al. [27] compared the mechanical properties of NFC and BC reinforced polymer nanocomposites by considering the plots of tensile strength against tensile modulus of both systems. A linear relationship was observed in the case of BC reinforced polymer nanocomposites, whereas that of the NFC reinforced polymer nanocomposites was more scattered. Tensile modulus and strength of BC (60 vol%) reinforced polymer nanocomposite were higher than those of NFC (90 vol%) reinforced polymer nanocomposites. Micromechanical models were also used to predict mechanical properties of both BC and NFC reinforced polymer nanocomposites. Negative deviation from the prediction was observed when the volume fraction of nanocellulose exceeds 10 vol%. This implies that the intrinsic high tensile stiffness of individual cellulose nanofibers has yet to be fully utilized.

In this study, thermomechanical and physical properties of the nanocellulose reinforced poly(vinyl alcohol) nanocomposites were of interest. Poly(vinyl alcohol) (PVA) was used as a model matrix for the preparation of nanocomposites due to its water solubility, easy process-ability, and transparency. BC and NFC reinforced poly(vinyl alcohol) composites were prepared using a solvent casting technique. A good interfacial adhesion and compatibility between cellulose nanofibers and the polymer matrix phase were presumed due to the fact that poly(vinyl alcohol) is also hydrophilic, as has been previously reported [11]. No study of the comparison between BC and NFC fibrils on physical, thermal, and mechanical properties of poly(vinyl alcohol) composites has been previously reported, to the best of authors' knowledge. The aim of this work is to investigate the effects of BC and NFC contents on thermal and mechanical properties of the polymer composites. The visible light transmittance of the composites was also measured and compared to the neat polymer resin. After all, it was expected that the knowledge obtained from this study, in terms of structure-properties relationships, will be useful for the further development of other related CNF/polymer nanocomposites. This includes the preparation of a transparent encapsulating film for solar cell modules with enhanced barrier properties from ethylene-vinyl acetate copolymer (EVA), which is an aspect of our future work.

2. Experimental

2.1. Chemicals. Partially hydrolyzed atactic poly(vinyl alcohol) (PVA) (98% hydrolysis, weight-average molecular weight 72,000 g mol^{-1}) was obtained from Fluka. Bacteria cellulose (BC) was obtained from the Kurabfood Co. Ltd. (Samut Songkhram, Thailand). It was purified by washing with boiling water for 10 min for three times before use. The final concentration of BC was 1% wt. Nanofibrillated cellulose (NFC), available in a form of sludge (10% wt in water), was purchased from the Daicel Finechem Ltd. (Tokyo, Japan). The NFC slurry was then further diluted with distilled water and stirred at room temperature for 24 h to make 1 wt% NFC suspension. Prior to blending with the polymer, both types of the nanofibers were disintegrated by a high speed blender at various times (10, 20, 30, 40, 50, and 60 min). It is noteworthy that, after mechanical treatment, appearance of the fibers was in a form of nonsettling turbidity in the supernatant (Figure 1). This indicates the presence of cellulose nanofiber as observed by Chen et al. [28] Morphology and average diameter values of the treated fibers were also examined by using a scanning electron microscope and an image analyzer. At least 20 fibers were randomly selected from several multiple SEM images of each sample, for the determination of the average diameter.

2.2. Preparation of PVA/Cellulose Nanofiber Composite Films. Pure PVA solutions were prepared by dissolving a given amount of PVA powder (from 1 to 10 wt%) directly in deionized water. To prepare the PVA/cellulose nanofibers (CNF) solution, the cellulose nanofibers were incorporated into PVA by adding a given amount of PVA powder to the

(a) (b)

Figure 1: Photographs of BC fibers (a) and NFC fibers (b) both before (left bottles) and after experienced mechanical treatment for 60 min (right bottles).

nanofiber aqueous solution and then we kept on stirring at 95°C for 2 h, until their complete dissolution [12]. The solution casted PVA/CNF nanocomposite film was then fabricated by pouring the solution into a Petri dish before drying at 60°C for 22 h or until reaching a constant weight. The thickness of the casted films was approximately 80 μm.

2.3. Spectroscopy Technique. The casted films were cut into a 5×5 cm^2 square shaped specimen and UV/Visible absorption spectra of various samples were recorded on a Shimadzu UV-3100 spectrophotometer over wavelengths ranging between 200 and 1000 nm. Visible light transmittance was determined in accordance with ISO 9050 standard method. The transmission of light through the polymer film was integrated over the wavelength range of 400–700 nm. Both total and diffuse light transmittance values were measured and reported. The linear light transmittance was also determined and reported by subtracting the total and diffuse values.

2.4. Microstructure and Morphology. A field emission gun scanning electron microscopy (FEG-SEM) technique was used to determine the diameter of the prepared fibers, using the (NOVA NANOSEM450, FEITM) machine. Prior to the SEM experiment, the SEM specimen was prepared as follows. The fiber suspension (1 wt%) was further diluted into a 0.0001 wt% aqueous solution. The solution was then dropped onto the SEM specimen stub and dried in an oven at 100°C, for 48 h, or until reaching a constant weight. The dried specimen was then coated with gold (Au) in order to avoid charging effect during the electron beam scanning, using a gold sputtering technique (SPI-moduleTM coater, S/N 10081).

The SEM experiment was operated with an accelerating voltage of 15 kV. In addition, morphology of various composites was also examined by using a JEOL (JSM 6610) machine, equipped with a secondary electron detector, using an accelerating voltage of 15 kV. The SEM specimens were prepared by fracturing of the rectangular test pieces, at 0°C, well below T_g of the PVA. Prior to the SEM experiment, the surfaces of the specimens were coated with gold (Au).

2.5. Mechanical Properties Test. The mechanical properties of the nanocomposites were determined using a universal testing machine (LLOYD; LR 50 K). Rectangular specimens (1 inch × 5 inches) were prepared by cutting the dried films with a die, in accordance with the ASTM D882 standard. The gauge length used was 50 mm and the tensile test was carried out at a crosshead speed of 500 mm min^{-1}, using the 1 kN load cell. At least five specimens were tested for each sample and the average values of Young's modulus, tensile strength at break, and elongation at break were calculated using standard equations and then reported. Tensile toughness was also calculated by using area underneath the stress-strain curve.

2.6. Thermal Properties Characterizations. The thermal behaviors of PVA and the various composites were determined using differential scanning calorimetry (DSC) (DSC 204 Cell/NETZSCH Thermal Analysis). The heating rate used was 10°C min^{-1} and the sample was scanned over temperatures ranging between 25°C and 250°C, under nitrogen gas atmosphere, using the sample weight of about 10 mg. Thermal stability of the polymer nanocomposites was also determined by thermal gravimetric analysis (TGA). The TGA experiment was carried out with a NETZSCH instrument (STA 409 PC/4/H Luxx Simultaneous TG DTA/DSC Apparatus). About 10 mg of the sample was used and the TGA experiment was scanned over temperatures ranging between 25°C and 600°C under nitrogen atmosphere, at a heating rate of 10°C min^{-1}.

3. Results and Discussion

3.1. Morphology of the Prepared Fibers. Figure 2 shows FEG-SEM images of the cellulose nanofibers, prepared under different mechanical treatment times. At the beginning (short treatment time), network-like structure forms on the surface of NFC were observed. As the mechanical treatment time was increased, more fiber network underneath was developed. The diameter of the fibers is relatively small as compared to their length, implying that the cellulose nanofibers are of high aspect ratios. However, due to an intrinsic continuous alignment of the fiber network, length of the fiber cannot be determined from these images. The average diameter values of BC and NFC determined from the SEM images using an image analyzer program are illustrated in Figure 3. It can be seen that the diameter values of both fibers decreased significantly after experiencing the mechanical treatment process (high speed blending). This indicates that the fibers

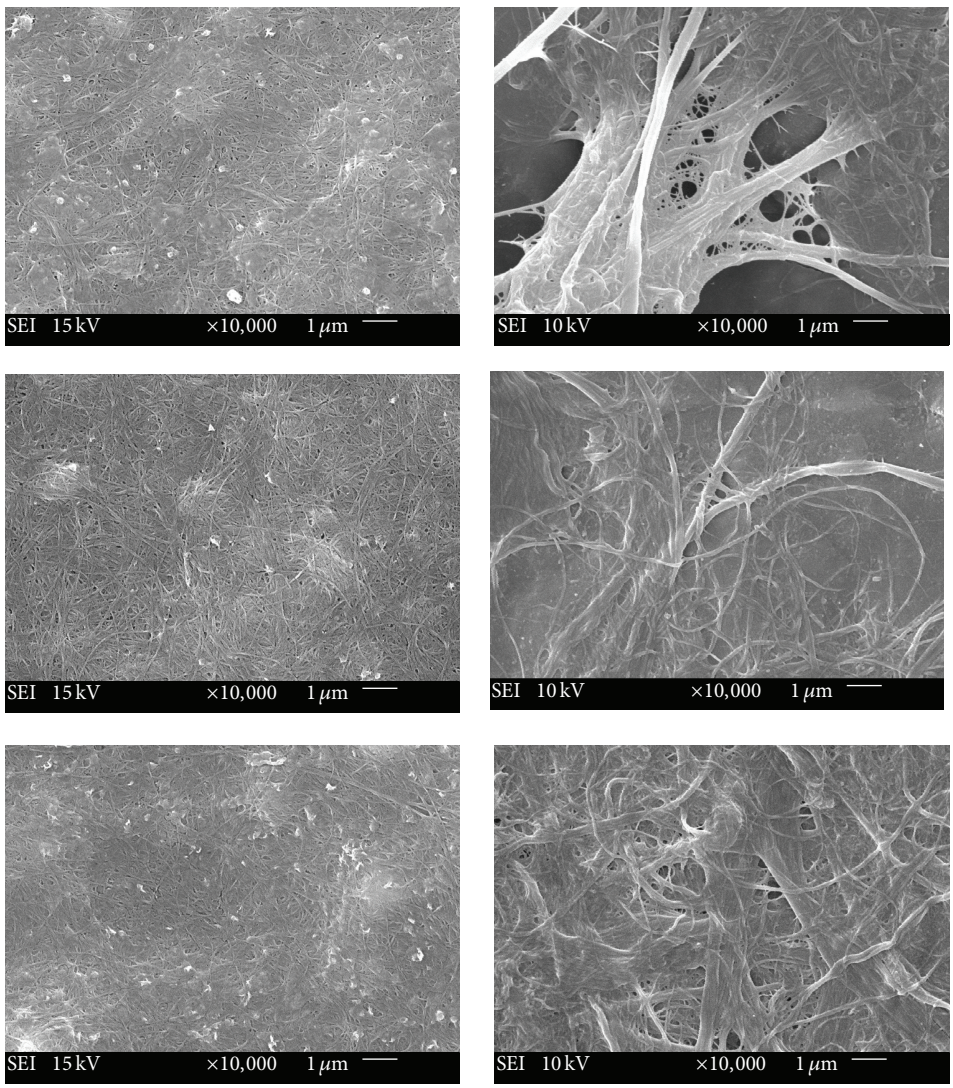

Figure 2: FE-SEM images of BC (left column) and NFC (right column) after experiencing a mechanical treatment for 10 min (top row), 30 min (middle row), and 50 min (bottom row).

have been disintegrated. The average diameter value of BC decreased from 1.371 μm to 0.049 μm after blending for 20 min. After that, the diameter gradually decreased with time. For example, the average diameter values of PVA/BC that experienced the treatment for 30, 50, and 60 min were found to be 0.049 (±0.01), 0.043 (±0.01), and 0.044 (±0.01) μm, respectively. Similarly, the diameter values of NFC fibers decreased rapidly with the mechanical treatment time during the first 20 min, beyond which the diameter slowly changed with time. Therefore, in this study, the BC and NFC prepared by mechanically treating the fiber for 60 min were used for further mixing with poly(vinyl alcohol) to fabricate nanocomposite films.

3.2. Mechanical Properties of the Composite Films. Tensile parameters were calculated and changes in tensile properties of the PVA with fiber type and content are illustrated in Figures 4–6. Regardless of the fiber types, tensile modulus of the composite increased with fiber content at the expense of their percentage elongation values. For example, modulus of the neat PVA specimen increased from 126 MPa to above 260 MPa after 6–10% wt of BC fibers was added. Likewise, after adding 8% wt of NFC, modulus of the PVA composite increased to about 200 MPa. This was due to reinforcing effect of the fibers in PVA [29]. The fibers are expected to be well compatible with PVA matrix due to the fact that both PVA and the fibers surface contain hydroxyl functional groups and the hydrogen bonding between phases can occur. This interaction might induce an effective stress transfer from the matrix to CNF and the better mechanical properties can be obtained. The above effect was absent in the case of the neat PVA specimen. From Figures 4–6, it is also noteworthy that the mechanical properties of PVA composite containing BC are greater than the mechanical properties of PVA composite containing NFC fiber, provided that the same level of cellulose nanofibers was used. Tensile toughness of the polymer film increased with the BC fiber content. The PVA/BC composite films were also tougher as compared to the neat PVA film. The

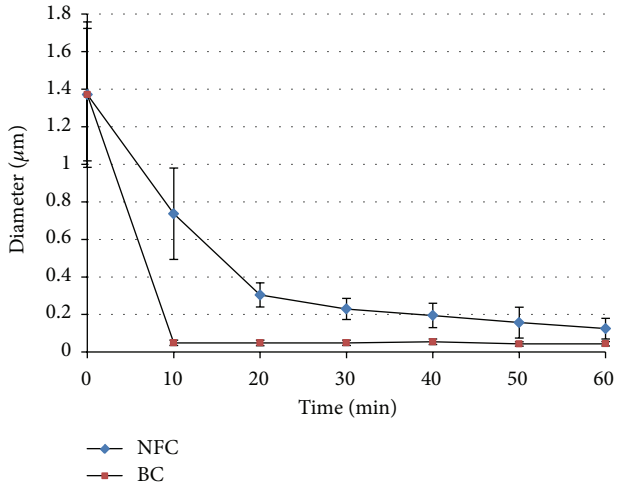

Figure 3: Changes in average diameter values of the cellulose fibers with the mechanical treatment time.

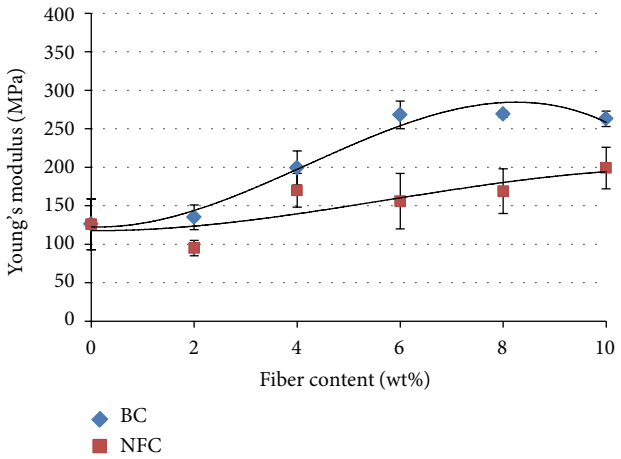

Figure 4: Young's modulus of various PVA nanocomposites containing different types and amounts of cellulose fiber.

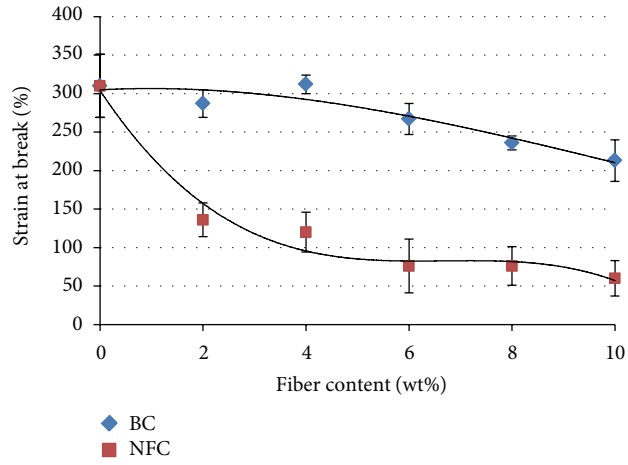

Figure 5: Percentage strain of various PVA nanocomposites containing different types and amounts of cellulose fiber.

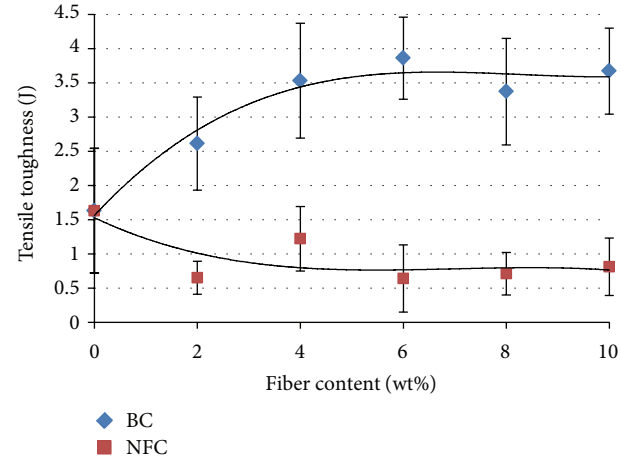

Figure 6: Tensile toughness of various PVA nanocomposites containing different types and amounts of cellulose fiber.

above results were similar to that reported by Lee et al. in a study on mechanical properties of cellulose nanofibers (CNF) reinforced epoxy resin [19]. In that case, tensile strength of BC reinforced epoxy nanocomposite was slightly greater than that of NFC reinforced epoxy nanocomposite, despite the fact that the former system contains lower nanocellulose loading. The effect was discussed in light of a critical surface energy of BC which is higher than that of NFC. Similarly, Nakagaito et al. [18] also studied mechanical properties of phenolic resin reinforced with BC sheet and found that tensile modulus values of the composites are superior to that of the MFC reinforced phenolic composites.

In our present study, it is worth mentioning that stress whitening was observed in all PVA/BC composites during the tensile test, regardless of the BC fiber content. The stress whitening of polymers is known to be attributed to formation of voids and/or intrinsic crazing. This could be induced by the presence of nanocellulose which, in turn, introduces heterogeneity into a polymer matrix. Due to significant differences in Young's modulus of the cellulose and the matrix, crazing could be created and the massive crazing contributed to the better tensile toughness of the PVA/BC composites. The above feature was, however, not the case for the PVA/NFC composites. It was because of the higher Young's modulus of single fibers for BC, compared to that of NFC. Work by Tanpichai et al. [4] showed that effective moduli of single fibril of BC and NFC were in the range of 79–88 and 29–36 GPa, respectively. It was believed that the difference is most likely due to the lower degree of crystallinity of the NFC as compared to that of BC [30].

3.3. Morphology of the Nanocomposites. Figure 7 shows SEM images of the tensile fractured surface of the various PVA composite films. It can be seen that surface roughness of the PVA/BC (2% wt) is greater than that of the PVA/NFC containing the same amount of fibers. By increasing the fiber content, surface roughness of the PVA/NFC (6% wt)

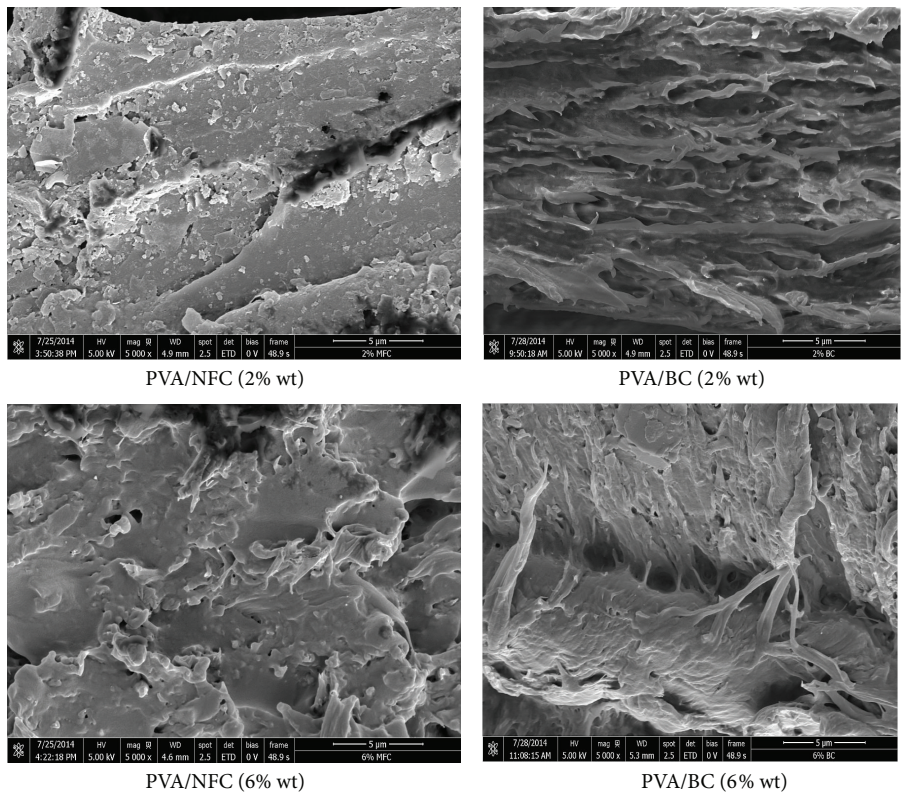

Figure 7: SEM images of tensile fractured PVA/cellulose nanofiber (CNF) composite specimens containing different types and amounts of CNF.

slightly increased, whereas that of the PVA/BC (6% wt) shows more plastic or ductile deformation. This reflects that the PVA/NFC nanocomposites were more brittle than that of the PVA/BC systems. The above statement was in a good agreement with the results from tensile test (Figures 3–6) and that can be explained in a similar fashion. Attempts were also made to examine the presence of cellulose nanofibers (CNF) within the PVA matrix from the cryofractured specimens. Results from Figure 8 show that CNF is well compatible with PVA, taking into account the fact that the fibers are well embedded within the polymer matrix and there is no gross phase separation or void formation at the interface. As the CNF content was further increased from 2% wt to 6% wt, trace evidence of the fiber cannot be clearly seen, especially for the PVA/BC system. In our opinion, this feature implies that the two phases became more miscible. This was probably attributed to a strong H-bonding interaction between two phases.

3.4. Thermal Behaviors. Changes in thermal behaviors of the polymer with fiber type and content should also be taken into account. Results from DSC thermograms (Figure 9) reveal that enthalpy of melting of PVA increased when 2% wt of cellulose nanofibers was added, regardless of the CNF type. This means that percentage crystallinity of PVA in the composites is greater than that of the neat PVA. This also implies that BC can act as a kind of the nucleating agent, enhancing crystallization rate and percentage of the crystallinity of PVA. Consequently, tensile modulus of the material increased. However, as the amount of CNF was further increased to 8 wt%, the enthalpy values were decreased again (Table 1). It seems that a capability of the fiber in acting as a nucleating agent dropped. Lu et al. [12] observed a slight increase of PVA crystallinity when a small amount (<5 wt%) of microfibrillated cellulose was added. At the high fibers loading, it was probable that some fibers were aggregated, which resulted in a lower interfacial area between PVA and the CNF. Thermal stability of PVA nanocomposites was also examined by using a thermalgravimetric analysis (TGA). According to the thermograms (Figures 10 and 11), three major transitions can be noted. The first transition occurred

Table 1: Enthalpy of melting of the various PVA nanocomposite films.

Materials	Fibers content (% wt)	T_m (°C)	Enthalpy (J/g)
PVA	—	213.0	46.10
PVA/BC	2	221.0	63.78
	4	219.5	62.61
	6	211.8	42.91
	8	209.7	26.51
PVA/NFC	2	219.0	70.70
	4	212.5	58.06
	6	221.8	55.02
	8	217.6	44.21

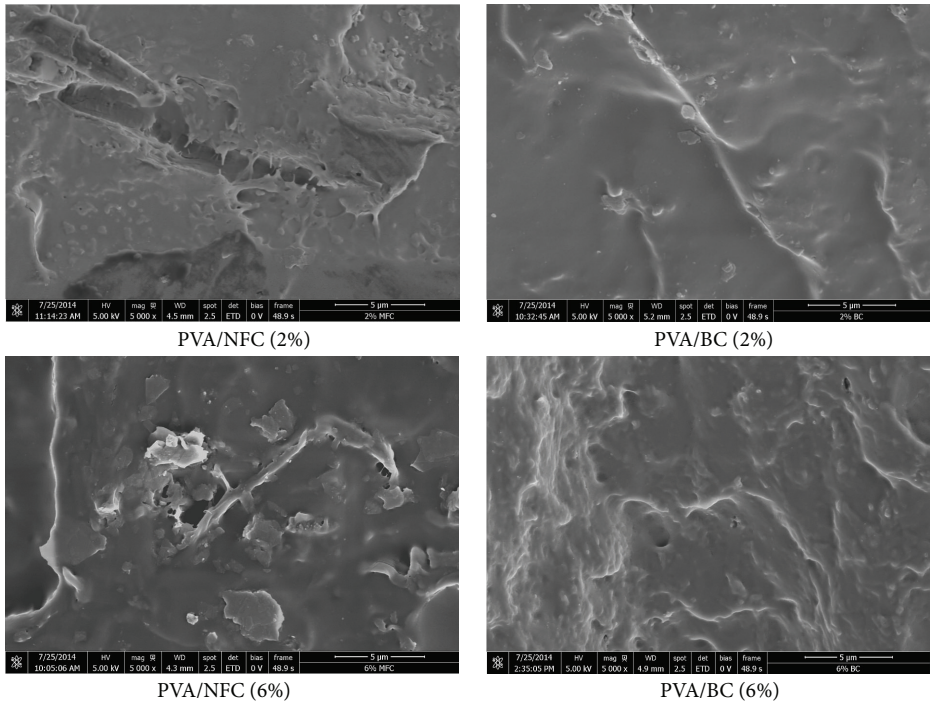

Figure 8: SEM images of cryofractured PVA/cellulose nanofiber (CNF) composite specimens containing different types and amounts of CNF.

Table 2: Percentage transmittance values of the various PVA nanocomposite films.

Materials		Transmittance* (%)		
Sample name	Fibers content (% wt)	Linear transmittance	Diffuse transmittance	Total transmittance
PVA	0	62.62	28.97	91.59
PVA/BC	2	76.14	14.94	91.08
PVA/BC	4	72.08	18.36	90.44
PVA/BC	6	74.52	15.92	90.44
PVA/BC	8	66.99	23.71	90.70
PVA/BC	10	68.92	21.47	90.39
PVA/NFC	2	76.37	14.75	91.12
PVA/NFC	4	51.97	38.29	90.26
PVA/NFC	6	61.69	28.02	89.71
PVA/NFC	8	53.84	34.62	88.46
PVA/NFC	10	48.63	38.53	87.16

*Visible range.

over the temperature ranging between 90 and 130°C and that can be ascribed to the evaporation of water adsorbed on the surface of the specimen. The second transition, which accounted for about 65% of weight loss, occurred over the temperature ranging between 240 and 330°C. This transition is predominately the characteristic degradation of PVA via dehydration (or elimination of water from the PVA molecules), which resulted in the formation of polyene intermediate. Finally, if the temperature was further increased above 420°C, the polyene intermediate undergoes a further chain scission, cyclization, and molecular decomposition, which resulted in the formation of residual solid or char. Notably, the onset degradation temperature (T_d) of both PVA/BC and PVA/NFC nanocomposites slightly increased as compared to that of the neat PVA. The similar effect was observed by Frone et al. [31] in a study on microcrystalline cellulose reinforced PVA. It is also worth mentioning that no further attempts were made to examine thermal behaviors of the PVA nanocomposites containing 10 wt% of the fibers. This was due to the fact that, at this high fiber content, no further improvement in terms of tensile toughness of the polymer composite films can be expected.

3.5. Optical Properties. Percentage visible light transmittance values of PVA nanocomposites containing different types and amounts of fibers are also calculated and summarized in Table 2. It was found that the total light transmittance of PVA composite films only slightly decreased after adding the

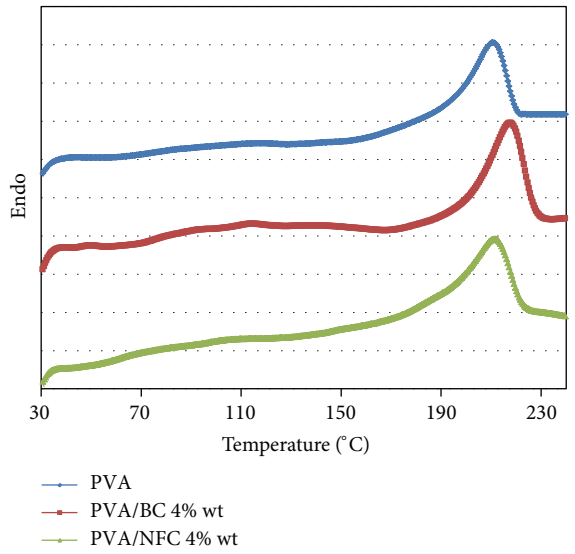

Figure 9: DSC thermograms of PVA and PVA nanocomposites containing 4 wt% of cellulose nanofiber.

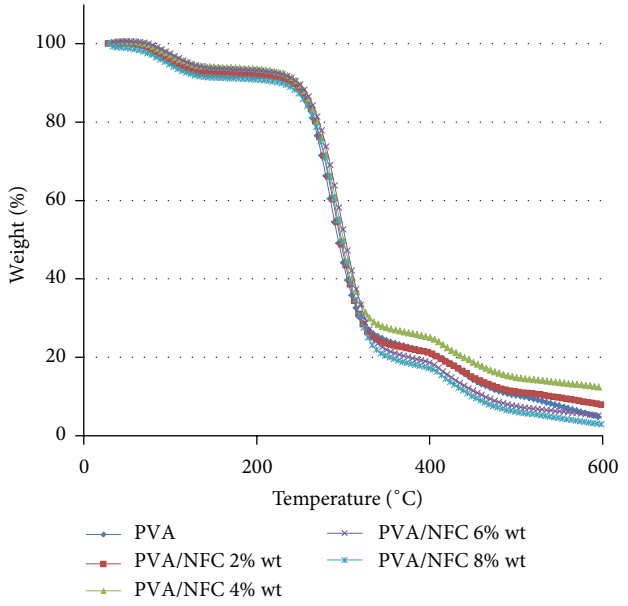

Figure 10: TGA thermograms of PVA/NFC nanocomposites.

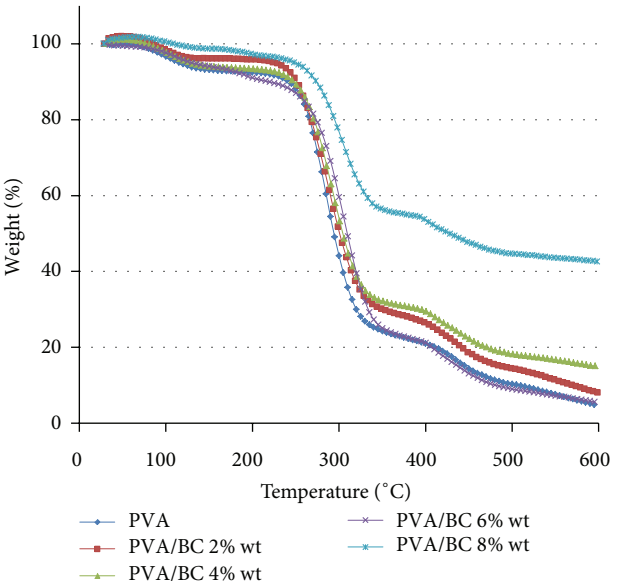

Figure 11: TGA thermograms of PVA/BC nanocomposites.

CNF, regardless of the fiber content. The above results could be attributed to the fact that both types of the CNF are also inherently semitransparent. Besides, the averaged diameter of the cellulose fibers, ranging between 40 and 180 nm, is considerably small as compared to the wavelength of visible light. The similar result was observed by Yano et al. [23] in a study on the optical property of BC reinforced epoxy composite. Consideration of percentage linear transmittance values of the two composite systems revealed that the values of the PVA/BC were greater than those of the (PVA/NFC), provided that the same level of fiber loading was used. In other words, percentage diffuse transmittance values of PVC/NFC were higher than those of PVA/BC. This implies that the path of light beam changes direction many times as it passes through the sample. In other words, there was more scattering of light inside the PVA/NFC samples. This was probably attributed to the higher diameter of the prepared NFC (Figure 3). Apart from that, the actual fiber length and the degree of dispersion of each fiber in the PVA matrix also play role. Further work has yet to be carried out in order to clarify this issue. Nevertheless, the total transmittance values in the visible region of all composite films are greater than 90%, regardless of the fiber type. The composite films apparently remain transparent (Figure 12). Our results suggest that it was possible to enhance mechanical and thermal properties of PVA, without scarifying large visible light transparency, by blending it with a suitable type and content of the cellulose nanofibers. More applications of the cellulose nanofibers can be extended by blending them with another transparent polymer matrix. This includes the development of ethylene vinyl acetate copolymer (EVA)/cellulose fiber nanocomposite films for use as a high performance solar cell encapsulant. This is an aspect of our future work.

4. Conclusions

Mechanical, thermal, and optical properties of poly(vinyl alcohol) (PVA) nanocomposites containing two different types of cellulose nanofibers (CNF), which are bacterial cellulose (BC) and nanofibrillated cellulose (NFC), were investigated. Tensile toughness of the PVA nanocomposites containing BC was found to be superior to those of the system containing NFC. The results were related to the differences between the two fibers in terms of an average diameter and their intrinsic properties. A capability of both types of CNF in acting as a nucleating agent for PVA was evidenced from the DSC thermograms and that contributed to the enhanced

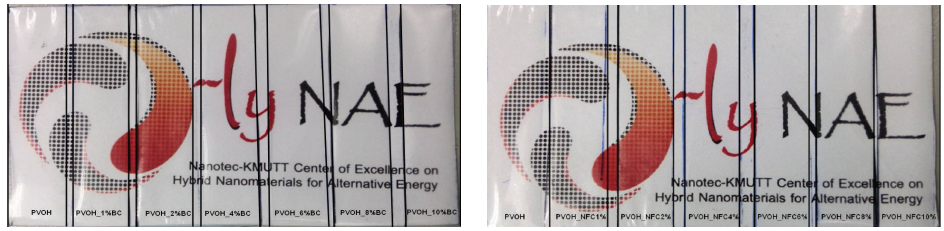

(a) (b)

Figure 12: Photographs showing transparency of the PVA/cellulose nanofiber composite films; PVA/BC (a) and PVA/NFC (b).

mechanical properties of the polymer nanocomposites. Thermal stability of PVA nanocomposites was also increased as compared to that of the neat PVA. Percentage visible light transmittances of the nanocomposite films were higher than 90%, regardless of the fiber type and content. Overall, in this study, we found that BC fibers have a better efficiency than NFC, in terms of reinforcing the poly(vinyl alcohol).

Conflict of Interests

The authors declare that there is no conflict of interests regarding the publication of this paper.

Acknowledgment

This work has been supported by the Nanotechnology Center (NANOTEC), NSTDA, Ministry of Science and Technology, Thailand, through its program of Center of Excellence Network.

References

[1] N. Lavoine, I. Desloges, A. Dufresne, and J. Bras, "Microfibrillated cellulose—its barrier properties and applications in cellulosic materials: a review," *Carbohydrate Polymers*, vol. 90, no. 2, pp. 735–764, 2012.

[2] X. Xu, F. Liu, L. Jiang, J. Y. Zhu, D. Haagenson, and D. P. Wiesenborn, "Cellulose nanocrystals vs. Cellulose nanofibrils: a comparative study on their microstructures and effects as polymer reinforcing agents," *ACS Applied Materials and Interfaces*, vol. 5, no. 8, pp. 2999–3009, 2013.

[3] I. Siró and D. Plackett, "Microfibrillated cellulose and new nanocomposite materials: a review," *Cellulose*, vol. 17, no. 3, pp. 459–494, 2010.

[4] S. Tanpichai, F. Quero, M. Nogi et al., "Effective young's modulus of bacterial and microfibrillated cellulose fibrils in fibrous networks," *Biomacromolecules*, vol. 13, no. 5, pp. 1340–1349, 2012.

[5] F. Quero, M. Nogi, H. Yano et al., "Optimization of the mechanical performance of bacterial cellulose/poly(L-lactic) acid composites," *ACS Applied Materials & Interfaces*, vol. 2, no. 1, pp. 321–330, 2010.

[6] S. J. Eichhorn, A. Dufresne, M. Aranguren et al., "Current international research into cellulose nanofibres and nanocomposites," *Journal of Materials Science*, vol. 45, no. 1, pp. 1–33, 2010.

[7] W. Chen, K. Abe, K. Uetani, H. Yu, Y. Liu, and H. Yano, "Individual cotton cellulose nanofibers: pretreatment and fibrillation technique," *Cellulose*, vol. 21, no. 3, pp. 1517–1528, 2014.

[8] M. Jonoobi, Y. Aitomäki, A. P. Mathew, and K. Oksman, "Thermoplastic polymer impregnation of cellulose nanofibre networks: morphology, mechanical and optical properties," *Composites Part A: Applied Science and Manufacturing*, vol. 58, pp. 30–35, 2014.

[9] T. Saito, R. Kuramae, J. Wohlert, L. A. Berglund, and A. Isogai, "An ultrastrong nanofibrillar biomaterial: the strength of single cellulose nanofibrils revealed via sonication-induced fragmentation," *Biomacromolecules*, vol. 14, no. 1, pp. 248–253, 2013.

[10] M. Bulota, K. Kreitsmann, M. Hughes, and J. Paltakari, "Acetylated microfibrillated cellulose as a toughening agent in poly(lactic acid)," *Journal of Applied Polymer Science*, vol. 126, no. 1, pp. E448–E457, 2012.

[11] S. Tanpichai, W. W. Sampson, and S. J. Eichhorn, "Stress-transfer in microfibrillated cellulose reinforced poly(lactic acid) composites using Raman spectroscopy," *Composites Part A: Applied Science and Manufacturing*, vol. 43, no. 7, pp. 1145–1152, 2012.

[12] J. Lu, T. Wang, and L. T. Drzal, "Preparation and properties of microfibrillated cellulose polyvinyl alcohol composite materials," *Composites Part A: Applied Science and Manufacturing*, vol. 39, no. 5, pp. 738–746, 2008.

[13] S. Iwamoto, S. Yamamoto, S.-H. Lee, and T. Endo, "Mechanical properties of polypropylene composites reinforced by surface-coated microfibrillated cellulose," *Composites Part A: Applied Science and Manufacturing*, vol. 59, pp. 26–29, 2014.

[14] A. Iwatake, M. Nogi, and H. Yano, "Cellulose nanofiber-reinforced polylactic acid," *Composites Science and Technology*, vol. 68, no. 9, pp. 2103–2106, 2008.

[15] A. N. Nakagaito and H. Yano, "Novel high-strength biocomposites based on microfibrillated cellulose having nano-order-unit web-like network structure," *Applied Physics A: Materials Science and Processing*, vol. 80, no. 1, pp. 155–159, 2005.

[16] A. Šturcováa, S. J. Eichhorn, and M. C. Jarvis, "Vibrational spectroscopy of biopolymers under mechanical stress: processing cellulose spectra using bandshift difference integrals," *Biomacromolecules*, vol. 7, no. 9, pp. 2688–2691, 2006.

[17] G. Guhados, W. Wan, and J. L. Hutter, "Measurement of the elastic modulus of single bacterial cellulose fibers using atomic force microscopy," *Langmuir*, vol. 21, no. 14, pp. 6642–6646, 2005.

[18] A. N. Nakagaito, S. Iwamoto, and H. Yano, "Bacterial cellulose: the ultimate nano-scalar cellulose morphology for the production of high-strength composites," *Applied Physics A: Materials Science and Processing*, vol. 80, no. 1, pp. 93–97, 2005.

[19] K.-Y. Lee, T. Tammelin, K. Schulfter, H. Kiiskinen, J. Samela, and A. Bismarck, "High performance cellulose nanocomposites: comparing the reinforcing ability of bacterial cellulose and nanofibrillated cellulose," *ACS Applied Materials & Interfaces*, vol. 4, no. 8, pp. 4078–4086, 2012.

[20] Y.-C. Hsieh, H. Yano, M. Nogi, and S. J. Eichhorn, "An estimation of the Young's modulus of bacterial cellulose filaments," *Cellulose*, vol. 15, no. 4, pp. 507–513, 2008.

[21] I. Sakurada, Y. Nukushina, and T. Ito, "Experimental determination of the elastic modulus of crystalline regions in oriented polymers," *Journal of Polymer Science*, vol. 57, no. 165, pp. 651–660, 1962.

[22] T. Nishino, K. Takano, K. Nakamae et al., "Elastic modulus of the crystalline regions of cellulose triesters," *Journal of Polymer Science, Part B: Polymer Physics*, vol. 33, no. 4, pp. 611–618, 1995.

[23] H. Yano, J. Sugiyama, A. N. Nakagaito et al., "Optically transparent composites reinforced with networks of bacterial nanofibers," *Advanced Materials*, vol. 17, no. 2, pp. 153–155, 2005.

[24] G. Siaueira, J. Bras, and A. Dufresne, "Cellulose whiskers versus microfibrils: influence of the nature of the nanoparticle and its surface functionalization on the thermal and mechanical properties of nanocomposites," *Biomacromolecules*, vol. 10, no. 2, pp. 425–432, 2009.

[25] G. Gong, J. Pyo, A. P. Mathew, and K. Oksman, "Tensile behavior, morphology and viscoelastic analysis of cellulose nanofiber-reinforced (CNF) polyvinyl acetate (PVAc)," *Composites Part A: Applied Science and Manufacturing*, vol. 42, no. 9, pp. 1275–1282, 2011.

[26] T. Zimmermann, E. Pöhler, and T. Geiger, "Cellulose fibrils for polymer reinforcement," *Advanced Engineering Materials*, vol. 6, no. 9, pp. 754–761, 2004.

[27] K. Y. Lee, Y. Aitomäki, L. A. Berglund, K. Oksman, and A. Bismarck, "On the use of nanocellulose as reinforcement in polymer matrix composites," *Composites Science and Technology*, vol. 105, pp. 15–27, 2014.

[28] W. Chen, H. Yu, Y. Liu, P. Chen, M. Zhang, and Y. Hai, "Individualization of cellulose nanofibers from wood using high-intensity ultrasonication combined with chemical pretreatments," *Carbohydrate Polymers*, vol. 83, no. 4, pp. 1804–1811, 2011.

[29] D. Bondeson and K. Oksman, "Polylactic acid/cellulose whisker nanocomposites modified by polyvinyl alcohol," *Composites Part A: Applied Science and Manufacturing*, vol. 38, no. 12, pp. 2486–2492, 2007.

[30] C. Aulin, M. Gällstedt, and T. Lindström, "Oxygen and oil barrier properties of microfibrillated cellulose films and coatings," *Cellulose*, vol. 17, no. 3, pp. 559–574, 2010.

[31] A. N. Frone, D. M. Panaitescu, D. D. Spataru, C. Radovici, R. Trusca, and R. Somoghi, "Preparation and characterization of PVA composites with cellulose nanofibers obtained by ultrasonication," *BioResources*, vol. 6, no. 1, pp. 487–512, 2011.